PERGAMON

International Journal of Heat and Mass Transfer 43 (2000) 1187–1199

International Journal of HEAT and MASS TRANSFER

www.elsevier.com/locate/ijhmt

Some experimental investigations on the concentration variance and its dissipation rate in a grid generated turbulent flow

F. Lemoine*, Y. Antoine, M. Wolff, M. Lebouche

LEMTA, 2, Avenue de la Forêt de Haye, BP 160, F-54504 Vandoeuvre-les-Nancy Cedex, France

Received 8 February 1999; received in revised form 27 May 1999

Abstract

This paper is devoted to an experimental investigation of concentration variance diffusion in a grid generated turbulent flow. Combined laser-induced fluorescence applied to concentration measurement and two-dimensional laser-Doppler velocimetry are implemented in order to measure simultaneously and instantaneously the molecular concentration of the passive tracer and two components of the carrier flow velocity. The different terms of the scalar variance transport equation can be measured directly in order to deduce the scalar fluctuations dissipation rate. It is shown that the approximation scalar variance advection $\simeq$ dissipation is valid, similarly to the decay of turbulent kinetic energy in the wake of a grid. The simultaneous determination of both scalar variance and kinetic energy dissipation rates permit an experimental determination of the scalar to velocity time scale ratio. Finally, an analysis of the self similarity of the fluctuating concentration field is also provided.

1. Introduction

The investigation of the diffusion of a passive scalar such as concentration in a steady turbulent flowfield requires a fine analysis of the mean and fluctuating concentration fields. The importance of the fluctuating concentration field is revealed in the mixing processes with possible chemical reactions or in air pollution problems where the maxima or the persistence of a given concentration are useful parameters [1]. This article is mainly devoted to the variance of concentration fluctuations of a passive contaminant, issuing from a point source and diffusing in a statistically homogeneous and isotropic turbulent flowfield. The measurement of the dissipation rate of the concentration fluctuations variance ε_c defined by:

$$\varepsilon_c = \sigma \overline{\frac{\partial c}{\partial x_i}\frac{\partial c}{\partial x_i}} \tag{1}$$

may allow the determination of the scalar dissipation scale, characterizing the interaction of the energy-containing eddies with the scalar field analogously to the Taylor microscale. In turbulent mixing processes, where chemical reactions are involved, the chemical reaction rate is governed by the scalar field dissipation microscale, which is related to the concentration fluctuations variance dissipation rate, as [2]:

$$\lambda_c^2 = \frac{12\sigma}{\varepsilon_c}\bar{c}^2 \tag{2}$$

* Corresponding author. Tel.: +33-03-83-59-57-32; fax: +33-03-83-59-55-44.

E-mail address: flemoine@ensem.u_nancy.fr (F. Lemoine).

0017-9310/00/$ - see front matter
PII: S0017-9310(99)00204-5

Nomenclature

C	molecular concentration
C_c	centerline molecular concentration
d	nozzle diameter
D_t	turbulent diffusivity
k	kinetic energy
g_i	gravitational acceleration
M	grid mesh
P	pressure
(r, Θ, x)	cylindrical coordinates
r_c	concentration profile half width radius
U_i	velocity component in the direction i
U	streamwise velocity component
V	radial velocity component

Greek symbols

α	volumetric expansion coefficient
ε	kinetic energy dissipation rate
ε_c	scalar variance dissipation rate
$\eta = r/r_c$	non-dimensional radial distance
λ_c	scalar dissipation microscale
λ_u	dynamic dissipation microscale
ν	kinematic viscosity
ρ	specific density
σ	molecular diffusivity

Other symbols

$*$	normalized values
X	instantaneous value of X
$\bar{X}$	averaged value of X
x	fluctuating part of X
$X = \bar{X} + x$	Reynolds decomposition

Moreover, Batchelor [3] has demonstrated that the passive scalar spectrum presents an inertial range analogous to the inertial range of the fluctuating velocity spectrum, where the properties of the spectrum depend only on the concentration variance dissipation rate ε_c and on the molecular diffusivity σ.

An other important point for improving the knowledge about the concentration variance dissipation rate is the closure problem of the transport equations of the passive scalar. In order to take into account the external forces like gravity, a second order closure of the turbulent mass flux must be considered [4,5]. The general equation governing the turbulent mass flux $\overline{u_i c}$ in a turbulent flowfield may be written as:

$$\frac{\partial \overline{u_i c}}{\partial t} + \bar{U}_j \frac{\partial \overline{u_i c}}{\partial x_j} = -\left(\overline{u_i u_j}\frac{\partial \bar{C}}{\partial x_j} + \overline{u_j c}\frac{\partial \bar{U}_i}{\partial x_j}\right) - \alpha \frac{\overline{c^2}}{\bar{C}} g_i + \overline{\frac{p}{\rho}\frac{\partial c}{\partial x_i}} - \frac{\partial}{\partial x_j}\left(\overline{u_i u_j c} + \frac{\overline{pc}}{\rho}\right) - (\sigma + \nu)\left(\overline{\frac{\partial c}{\partial x_j}\frac{\partial u_i}{\partial x_j}}\right) \quad (3)$$

where ρ is the fluid specific density, σ is the molecular diffusivity, ν is the kinematic viscosity, g_i is the gravitational acceleration and α is the dimensionless volumetric expansion coefficient. The term of mean squared concentration fluctuations appears directly in the buoyant source of the turbulent mass flux equation. The general equation governing the evolution of the mean squared concentration fluctuations may be written as [6]:

$$\frac{1}{2}\left(\frac{\partial \bar{c}^2}{\partial t} + \bar{U}_j \frac{\partial \overline{c^2}}{\partial x_j}\right) = -\overline{cu_j}\frac{\partial \bar{C}}{\partial x_j} - \frac{1}{2}\frac{\partial \overline{u_j c^2}}{\partial x_j} + \frac{1}{2}\sigma \frac{\partial^2 \overline{c^2}}{\partial x_j^2} - \varepsilon_c \quad (4)$$

One of the more important term, which requires a modelisation is the dissipation rate of the concentration variance ε_c. An usual way to determine ε_c is to use the scalar to velocity time scale ratio R, defined by:

$$R = \frac{\varepsilon q}{k \varepsilon_c} \quad (5)$$

where k is the kinetic turbulent energy, ε its dissipation rate and q is defined as $q = \frac{1}{2}\overline{c^2}$. However, numerous disagreements exist relevant to the value of the ratio R, which, according to Launder [6] may be not a universal constant and may strongly depend on the exact nature of the flowfield. An alternative way is to determine ε_c from its own transport equation. However, the discussion about the ε_c equation is open because of a lack of measurements of ε_c in simple flowfields [6].

Csanady [1] as Gibson and Schwarz [7] have assumed, for a homogeneous and isotropic turbulent flowfield, that the concentration variance dissipation rate is related to the decay law of the concentration fluctuations, similarly to the kinetic energy decay law in the wake of a grid. Moreover, a few authors such as Csanady [1] and Nakamura et al. [8] pointed out the self preservation of the concentration fluctuations variance in a grid generated turbulent flow. Nakamura et al. [8] checked experimentally this self-preservation with the help of mean and fluctuating concentration measurements of a diffusive passive contaminant.

However, no direct measurements of the turbulent mass flux $\overline{u_i c}$ and of the triple correlation $\overline{u_i c^2}$, both present in the scalar variance transport equation have been provided by these authors. The problem of the closure of the turbulent mass flux $\overline{u_i c}$ has been discussed by Lemoine et al., in a statistically homogeneous and quasi-isotropic turbulent flowfield [9,10]. The present paper provides direct measurements of the different terms of the concentration variance equation and discusses the orders of magnitude of these terms. The dissipation rate of the concentration variance is determined with the help of a budjet on the concentration variance transport equation. In order to perform these measurements, the laser-induced fluorescence technique, applied to the concentration measurement in liquid media has been implemented in order to measure mean and fluctuating concentration. Laser-induced fluorescence technique has been combined with the laser-Doppler velocimetry as described in the Refs. [9–12] in order to measure simultaneously and instantaneously, in the same sample volume the concentration (or temperature in Ref. [12]) and two-dimensional (2D) velocity fluctuations. By using this technique, the double and triple correlations $\overline{u_i c}$ and $\overline{u_i c^2}$ are accessible.

2. Flow conditions and experimental set-up

2.1. Flow conditions

The flowfield consists in a statistically homogeneous and quasi-isotropic turbulent flow, generated by means of a grid, in a square test channel. The characteristics of the test channel and of the grid are given in Ref. [10]. The passive contaminant is injected in the center of the test channel, at 280 mm downstream of the grid, by means of a round nozzle (Fig. 1). The injection velocity is similar to the turbulent flow velocity, in order to avoid shear effects. The mean flow velocity is about 1.65 m/s which corresponds to a mesh Reynolds number of 16,500. The measurements have been performed from $x/M = 38$ to $x/M = 52$ in the initial period of the decaying grid turbulence. The diameter of the injection nozzle has been reduced to 1 mm in order to limit the effects of the wake of the injection pipe. As shown in Ref. [10], the turbulent field can be considered as statistically homogeneous and quasi-isotropic, although a larger turbulence intensity observed on the streamwise component. The rate of turbulence is about 3% and the turbulence intensity decays downstream of the grid. The streamwise decay of turbulence, shown in Fig. 2, can be written as:

$$\frac{\bar{U}^2}{\overline{u^2}} = 1.574\left(\frac{x}{M}\right)^{1.66} \tag{6}$$

The dissipation rate of the kinetic turbulent energy can be inferred from the streamwise decay of kinetic energy (derivation of Eq. (6)):

$$\varepsilon = -\bar{U}\frac{\mathrm{d}k}{\mathrm{d}x} = \frac{3}{2}\bar{U}^3\frac{0.47}{M}\left(\frac{x}{M}\right)^{-2.66} \tag{7}$$

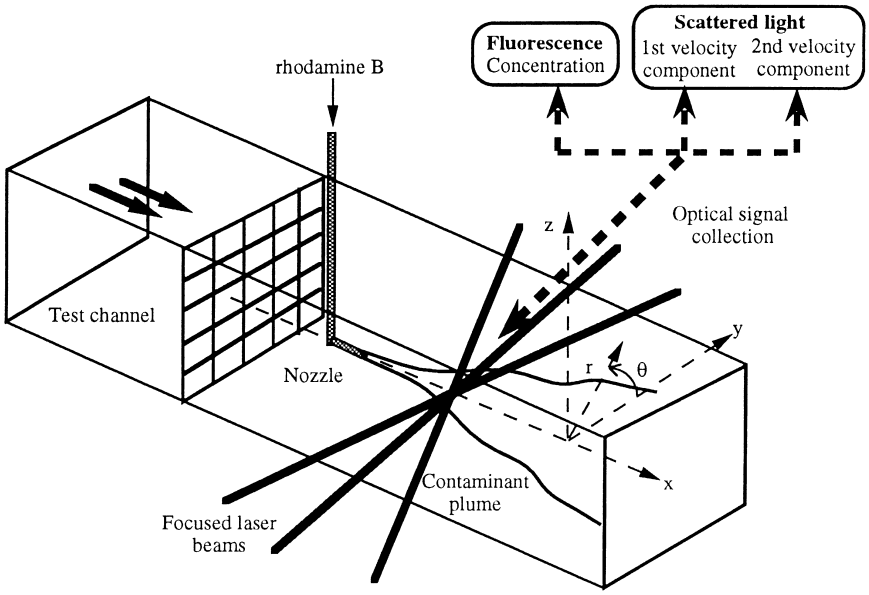

Fig. 1. Experimental arrangement.

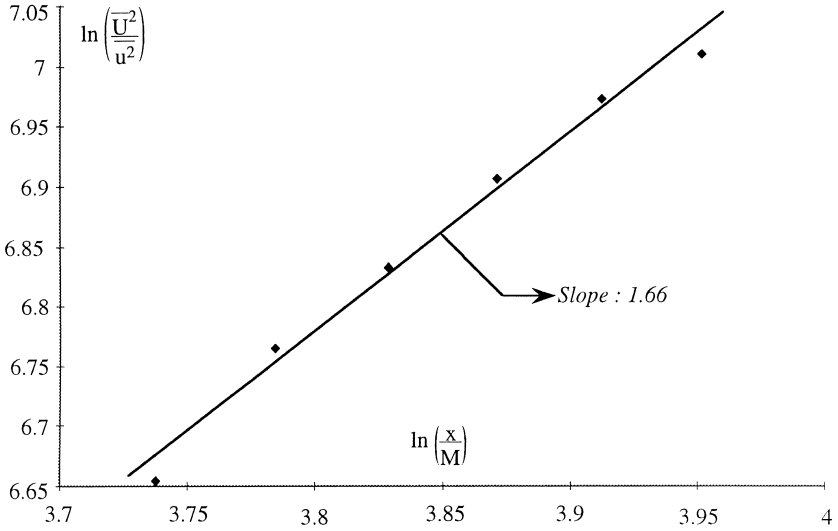

Fig. 2. Streamwise decay of turbulent kinetic energy.

2.2. Measurement set-up

Combined laser-induced fluorescence and 2D laser-Doppler velocimetry have been used in order to measure simultaneously and instantaneously in the same probe volume, the molecular concentration of the diffusive tracer and two components of the velocity. All the important features and details of the experimental measurement techniques are given in the Refs. [10,11]. The main component of the set-up is a 2D laser-Doppler velocimeter (DANTEC). The passive contaminant is a fluorescent organic dye, rhodamine B, highly diluted in water (molecular concentration, $C = 10^{-6}$ mol/l). The fluorescence of this dye can be efficiently induced by the green radiation ($\lambda = 514.5$ nm) of the argon-ion laser of the velocimeter. The emitted fluorescence is proportional to the molecular tracer concentration [11,13]. The optical signal is collected by means of an optical device, and is separated and filtered subsequently. The optical signal contains:

- the scattered light at $\lambda = 488$ nm (filtered by a dichroic blade),
- the scattered light at $\lambda = 514.5$ nm (filtered by a dichroic blade),
- the large-bandwidth fluorescence of rhodamine B (filtered by a high-pass filter, cut-off 550 nm).

The scattered light at $\lambda = 488$ and $\lambda = 514.5$ nm are separately converted to an electrical current by means of photomultiplier tubes and the Doppler signals are processed by fast Fourier transforms using Burst Spectrum Analyser (DANTEC), which provides a more accurate measurement than the frequency trackers used in Refs. [9,10]. The fluorescence intensity is measured by means of a photomultiplier tube, which provides an analogical signal, proportional to the concentration. The analogical signals, relevant to the velocity components and concentration are processed and correlated by means of a computer associated with a data acquisition board. Mean quantities, second-order moments, double and triple cross-correlations between concentration and velocity fluctuations are calculated with 50,000 samples using a 10 kHz sampling frequency.

3. Fluctuating concentration field

3.1. General concepts

In the case of a point source discharging in a statistically homogeneous and quasi-isotropic turbulent flow, the governing equation for the concentration fluctuations variance may be written using the boundary layer approximation, with the use of cylindric coordinates (Fig. 1):

$$\frac{1}{2}\bar{U}\frac{\partial\overline{c^2}}{\partial x} = -\overline{cv}\frac{\partial\bar{C}}{\partial r} - \frac{1}{r}\frac{\partial}{\partial r}\left(r\frac{\overline{vc^2}}{2}\right) - \varepsilon_c \tag{8}$$

All the terms of Eq. (8), e.g., quadratic means, double and triple correlations can be measured directly using combined LIF and LDV techniques, except the scalar fluctuations dissipation term ε_c which can be deduced by considering the budjet on Eq. (8).

3.2. Mean concentration field

The mean concentration field is well characterized by Gaussian self similar profiles in a statistically homo-

geneous turbulent flowfield, as shown Fig. 3 in normalized values. The concentration field can be expressed as [8,9]:

$$\bar{C}(x,\eta) = \bar{C}_c(x)e^{-\ln 2\eta^2} \tag{9}$$

where $\bar{C}_c(x)$ is the centerline concentration, and $\eta = r/r_c$, where r_c is the half width radius of the mean concentration profile. The streamwise expansion of the concentration plume, characterized by the half width radius r_c, is reported in Fig. 4 and follows a square root law as predicted by the theory [8]:

$$\left(\frac{r_c}{M}\right)^2 = 2.98\left(\frac{x}{M} - 29\right) \tag{10}$$

The streamwise decay of centerline mean concentration, also reported in Fig. 4, follows an hyperbolic law given by:

$$\frac{1}{C_c} \sim \left(\frac{x}{M} - 31\right) \tag{11}$$

3.3. Concentration variance and advection term

As shown in Fig. 5, the concentration variance profiles look like Gaussian. An initial concentration of rhodamine B exists in the test channel and a previous concentration measurement is performed without injection of the fluorescent tracer. Although this concentration can be considered as uniform, a fluctuating part is observed, due to the physical process of fluorescence itself, which follows a Poisson statistic [14].

The measured variance of uniform concentration existing in the test channel is subtracted to turbulent concentration variance. It can be also observed (Fig. 5) that the variance in the edges of the profiles is not reduced to zero, because the optical access is not large enough to investigate the entire profile. The variance profiles appear also self similar; the amplitude of the concentration variance $\bar{c}^2$ is reduced by its local centerline value and the radial distance by the concentration half width radius r_c. A significant scatter of the experimental data can be observed Fig. 5. It can be attributed to the strong Poisson noise of the fluorescence process itself and to the difficulty of injecting the passive tracer at the flow velocity. The decay law of the centerline value of the concentration variance, denoted by $(\overline{c^2})_c$, is reported in Fig. 6 and follows a square root law:

$$\frac{1}{\sqrt{(\overline{c^2})_c}} = 0.018\left(\frac{x}{M} - 24\right) \tag{12}$$

This result is compatible with the self-similarity analysis of the fluctuating concentration field developed in Section 4.

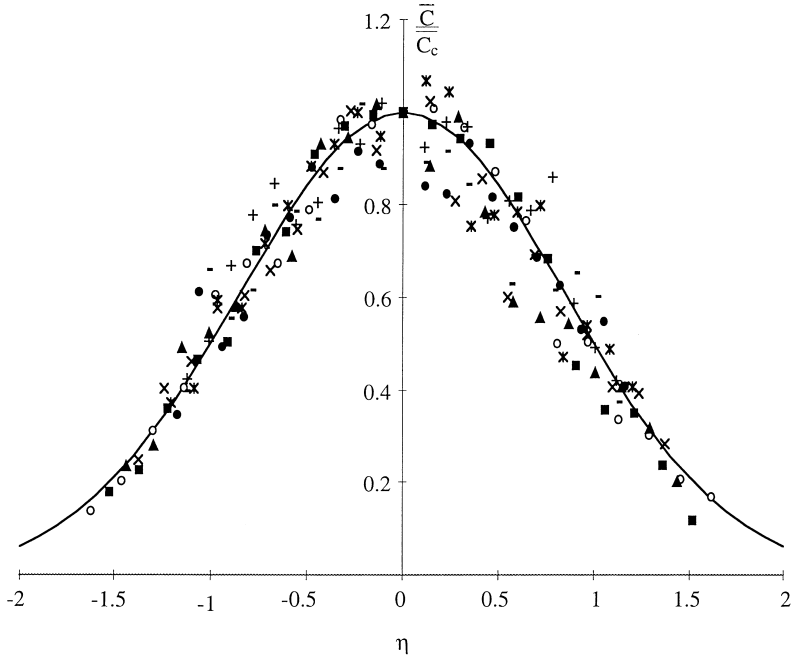

Fig. 3. Radial distribution of mean fluorescent tracer concentration. x/M: ○ 38; ■ 40; ▲ 42; × 44;* 46; • 48; + 50; – 52. ——— Gaussian fit.

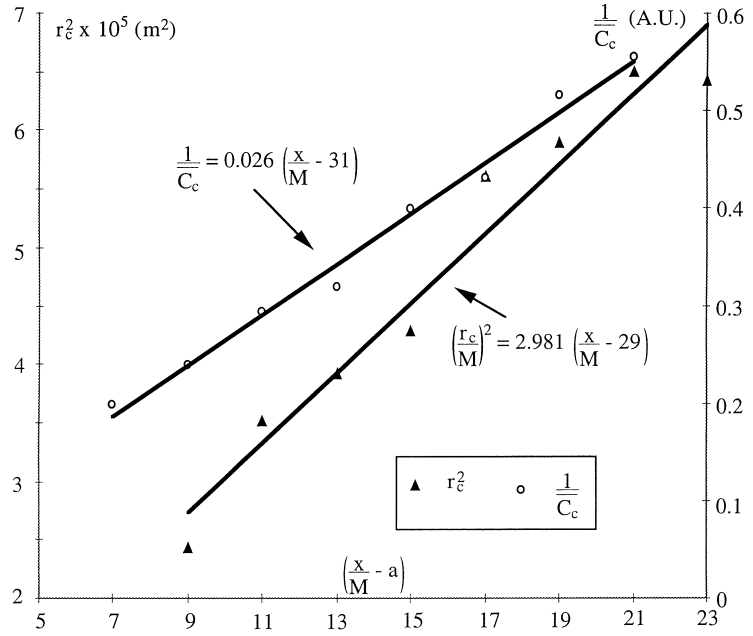

Fig. 4. Streamwise distribution of the expansion length scale of the mean concentration profile and centerline concentration.

In the light of the previous investigations, the concentration variance is given by the following self-similar law:

$$\overline{c^2}(x,\eta) = \left(\overline{c^2}\right)_c(x)g(\eta) \tag{13}$$

where $g(\eta)$ is a Gaussian type function. The advection term of the concentration variance (Eq. (8)) is given by:

$$\frac{1}{2}\bar{U}\frac{\partial\overline{c^2}}{\partial x} = \frac{1}{2}\bar{U}\left(\frac{\partial\left(\overline{c^2}\right)_c}{\partial x}g(\eta) - \frac{\left(\overline{c^2}\right)_c a\eta}{2r_c^2}\frac{\partial g(\eta)}{\partial\eta}\right) \tag{14}$$

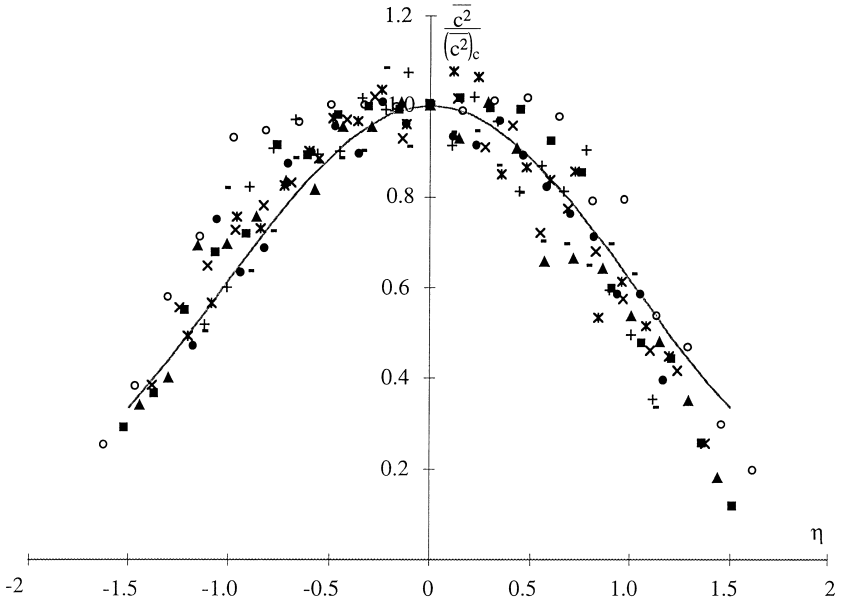

Fig. 5. Radial distribution of the concentration variance. x/M: ○ 38; ■ 40; ▲ 42; × 44; * 46; ● 48; + 50; – 52. ——— Numerical fit.

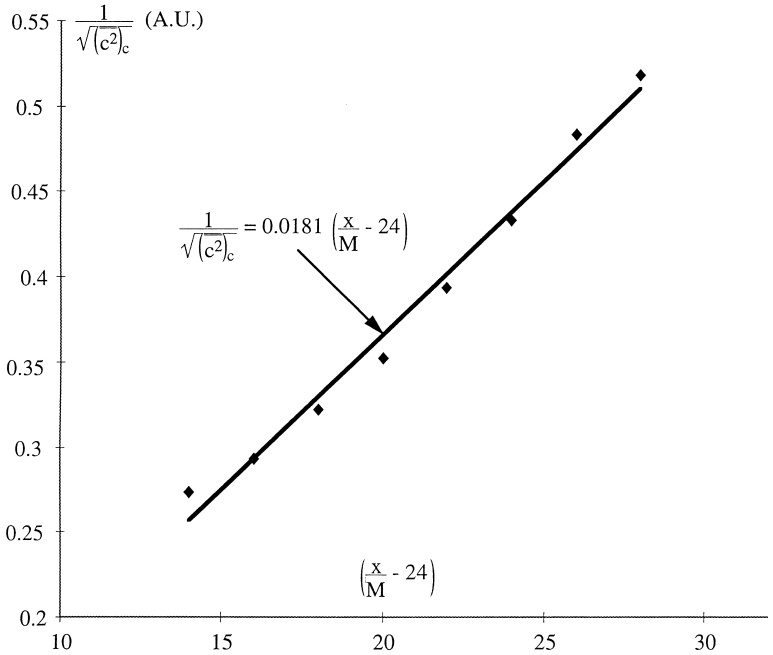

Fig. 6. Streamwise distribution of the centerline concentration variance.

where $a = \mathrm{d}r_c^2/\mathrm{d}x$ is a constant [8,9].

The advection term $\frac{1}{2}\bar{U}\frac{\partial \overline{c^2}}{\partial x}$ is determined by means of least squares fits of $(\overline{c^2})_c(x)$ and $g(\eta)$ using Eq. (14).

3.4. Production term

Both the elements of the production term $\overline{cv}(\partial \bar{C}/\partial r)$ term have been determined. The turbulent transverse mass flux has been measured and the mean concentration gradient is calculated by simple derivation of Eq. (9). Each $\overline{vc}$ profile (Fig. 7) has been normalized by its own maximum value denoted by $(\overline{vc})_{max}$ and the radial distance by the half width radius of concentration r_c:

$$\overline{vc}(x\eta) = (\overline{vc})_{max}(x)h(\eta) \tag{15}$$

The streamwise distribution of $(\overline{vc})_{max}(x)$ is reported in Fig. 8 and is fitted with a power law. The non-dimensional expression of $h(\eta)$ may be written as in Ref. [9], where $\overline{vc}$ is modeled with a constant turbulent diffusivity coefficient:

$$h(\eta) = \frac{-\eta \mathrm{e}^{-\ln 2\eta^2}}{\sqrt{\frac{1}{2\ln 2}}\mathrm{e}^{-1/2}} \tag{16}$$

3.5. Triple correlation $\overline{vc^2}$ and diffusion term

In the light of the experimental data, the triple correlation $\overline{vc^2}$ (Fig. 9) exhibits self-similar antisymmetric profiles as the double correlation $\overline{vc}$. The amplitude of $\overline{vc^2}$ is reduced by its maximum value, denoted by $(\overline{vc^2})_{max}$ and the radial distance by the half width radius r_c of the concentration profile. Consequently, with the help of the streamwise distribution of $(\overline{vc^2})_{max}$ reported in Fig. 10, the distribution of $\overline{vc^2}$ may be represented by:

$$\overline{vc^2}(x,\eta) = \left(\overline{vc^2}\right)_{max}(x)k(\eta) \tag{17}$$

Least squares fits of $(\overline{vc^2})_{max}(x)$ and $k(\eta)$ allows to calculate the diffusion term $\frac{1}{r}\frac{\partial}{\partial r}(r\frac{\overline{vc^2}}{2})$.

A closure of the triple correlation $\overline{vc^2}$, as a gradient-type representation has been suggested [15]:

$$-\overline{u_i c^2} = K_1 \frac{k}{\varepsilon}\overline{u_i u_j}\frac{\partial \overline{c^2}}{\partial x_j} \tag{18}$$

Under the present flow conditions and considering the boundary layer approximation, the triple correlation $\overline{vc^2}$ can be represented by:

$$-\overline{vc^2} = K_1 \frac{k}{\varepsilon}\bar{v}^2\frac{\partial \overline{c^2}}{\partial r} = A_t\frac{\partial \overline{c^2}}{\partial r} \tag{19}$$

It can be interpreted as a gradient model of the triple correlation and the coefficient $A_t = K_1\frac{k}{\varepsilon}\overline{v^2}$ as a turbulent diffusivity coefficient of the concentration variance. K_1 is a numerical constant, which needs to be adjusted in the light of experimental data. The parameters k

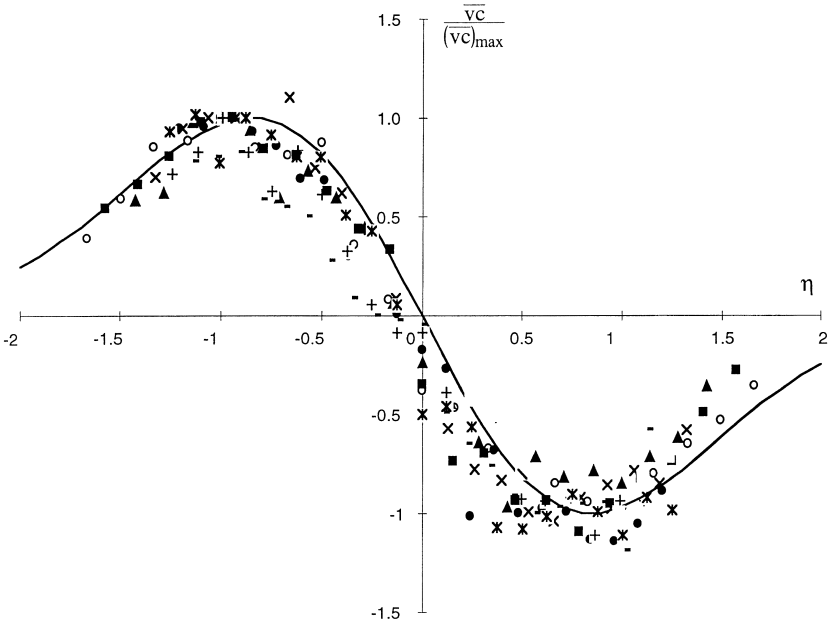

Fig. 7. Radial distribution of the turbulent mass flux in the transverse direction. x/M: ○ 38; ■ 40; ▲ 42; × 44; * 46; • 48; + 50; – 52. ——— Theoretical (turbulent diffusitivity model).

and ε representing the kinetic energy of turbulence and its dissipation rate can be easily evaluated using Eqs. (6) and (7) and the gradient term $\partial\overline{c^2}/\partial r$ is calculated using the present experimental data. The distribution

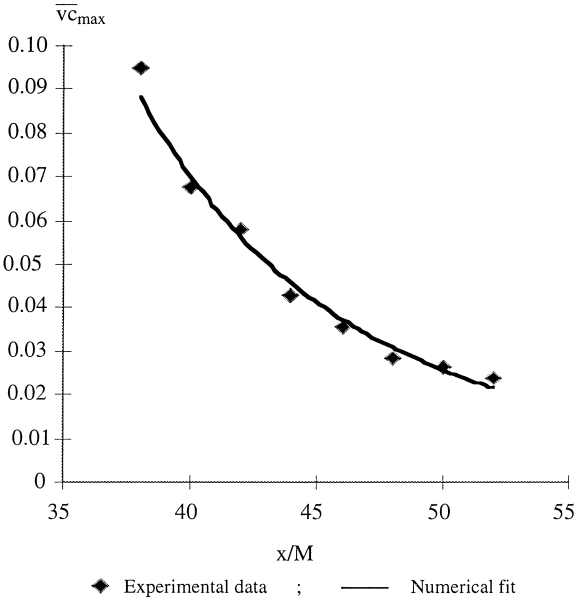

Fig. 8. Streamwise distribution of the maximum value of the $\overline{vc}$ cross-correlation. ◆ Experimental data; ——— numerical fit.

of A_t over a cross-section is reported in Fig. 11. The values of A_t have been calculated with the experimental data obtained for the triple correlation $\overline{vc^2}$ and the least squares fit of $\overline{c^2}$ in order to evaluate the radial gradient of the concentration variance. Although there is a significant scatter of the data, the coefficient A_t exhibits almost a constant value over the cross-section (for the cross-section at $x/M = 50$). For cross-sections closer to the injection point, constancy is reached only for $\eta > 0.16$. A value of $A_t = 1.7 \times 10^{-4}$ m^2/s can be considered. Moreover, the parameter A_t appears almost constant over the entire flowfield, in the initial period of the decaying grid turbulence, which allows us to determine the value of the numerical constant K_1. A value of $K_1 = 0.31$ has been determined.

3.6. Scalar variance and dissipation: budjet

The global budjet on the transport equation of the scalar variance $\overline{c^2}$ (Eq. (8)) is reported in Fig. 12, in normalized values. All the quantities presented in the budjet must be normalized by the mean velocity $\bar{U}$, the squared centerline concentration $(\overline{C^2})_c$ and by the length scale r_c. Most of the terms of this equation have been determined from the analysis of the experimental data, except the scalar variance dissipation rate ε_c, which can be inferred from the budjet on Eq. (8). In the light of Fig. 12, the diffusion and the production terms are negligible over the major part of the cross-section, compared to the dissipation and advection

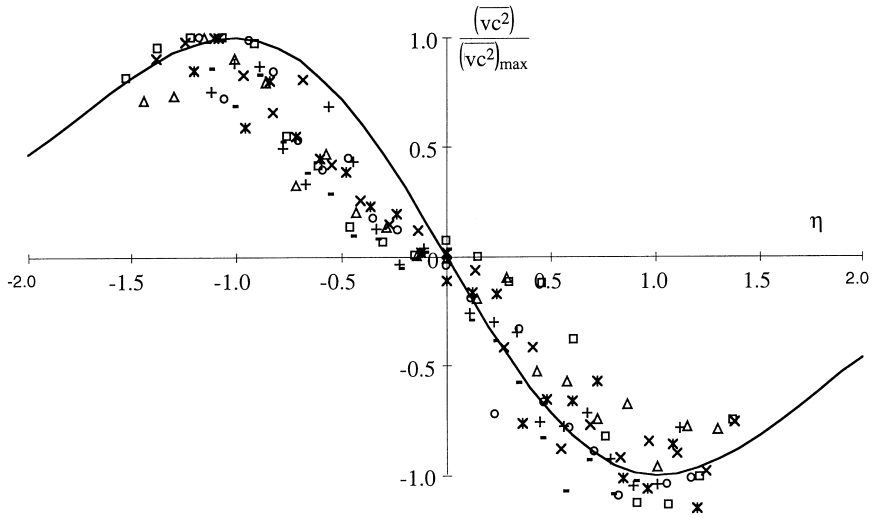

Fig. 9. Radial distribution of the triple correlation $\overline{vc^2}$. x/M: ○ 38; □ 40; △ 42; × 44; * 46; + 50; − 52. ——— Numerical fit.

terms. It demonstrates clearly that the approximation $\bar{U}\frac{\partial \overline{c^2}}{\partial r} \approx -\varepsilon_c$ is valid over the major part of the flowfield. This relation seems to be analogous to the decay of turbulent kinetic energy in the wake of a grid [7]. The distribution of the dissipation rate ε_c can be used in order to determine the scalar to velocity time scale ratio R defined by Eq. (5). As seen in Fig. 13, the time scale ratio R exhibits a quite constant value over the major part of the flowfield, except in the edges zones where the concentration is too low to be measured accurately. The numerical value of R is about 0.45, and a very low streamwise variation of R, exceeding not 2% between $x/d = 38$ and $x/d = 52$ is observed. Other authors have reported numerical values of the ratio R. Spadling [16] used $R = 0.5$ in turbulents jets, and Launder used $R = 0.8$ in turbulents shear flows.

3.7. Discussion

The validity of the distribution of ε_c inferred from the budjet on the concentration variance equation will be discussed. The different scales relevant to both inertial range of dynamic and scalar field will be considered. The inertial range of the dynamic field can be characterized by the Taylor microscale defined by:

$$\lambda_u^2 = 15\nu\frac{\overline{u^2}}{\varepsilon} \tag{20}$$

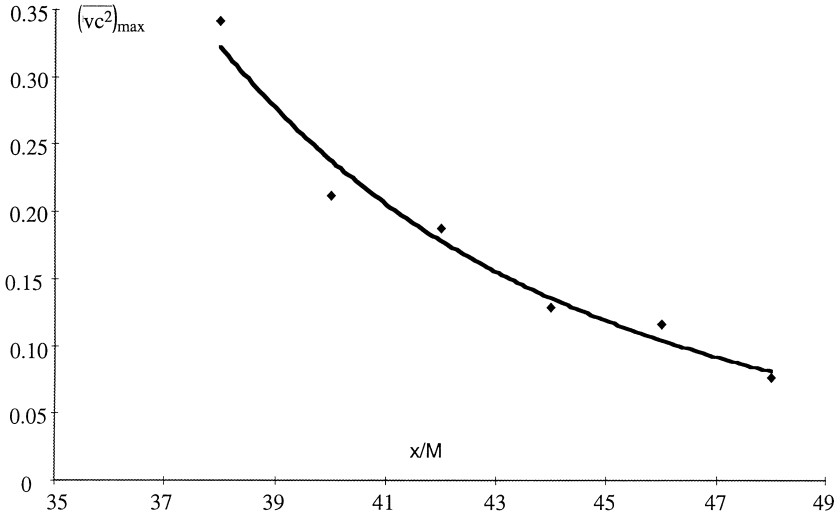

Fig. 10. Streamwise distribution of maximum value of the triple correlation $\overline{vc^2}$.

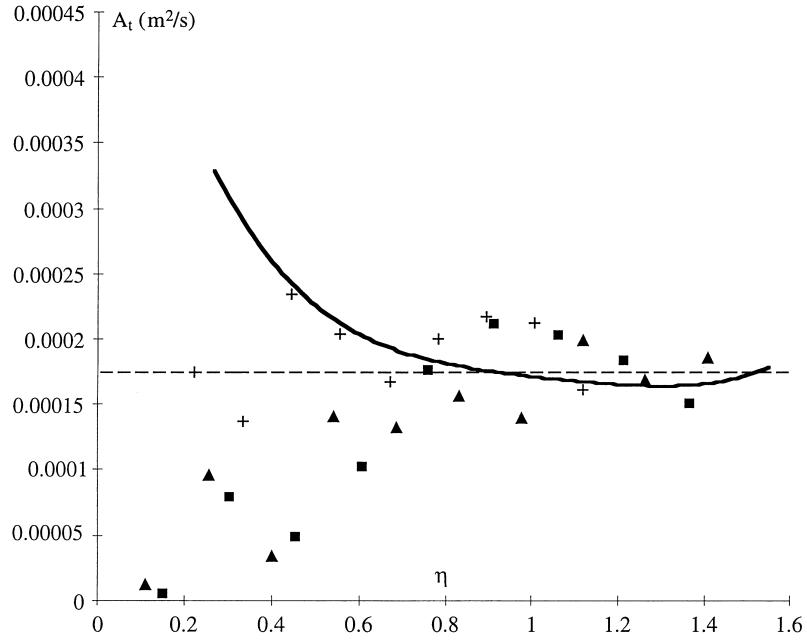

Fig. 11. Radial distribution of the diffusivity A_t. x/M: ■; △ 160; + 220. – – – A_t calculated with the constant ratio D_t/A_t. ——— A_t calculated with numerical fit of $\partial\overline{c^2}/\partial r$ and experimental data for $\overline{vc^2}$.

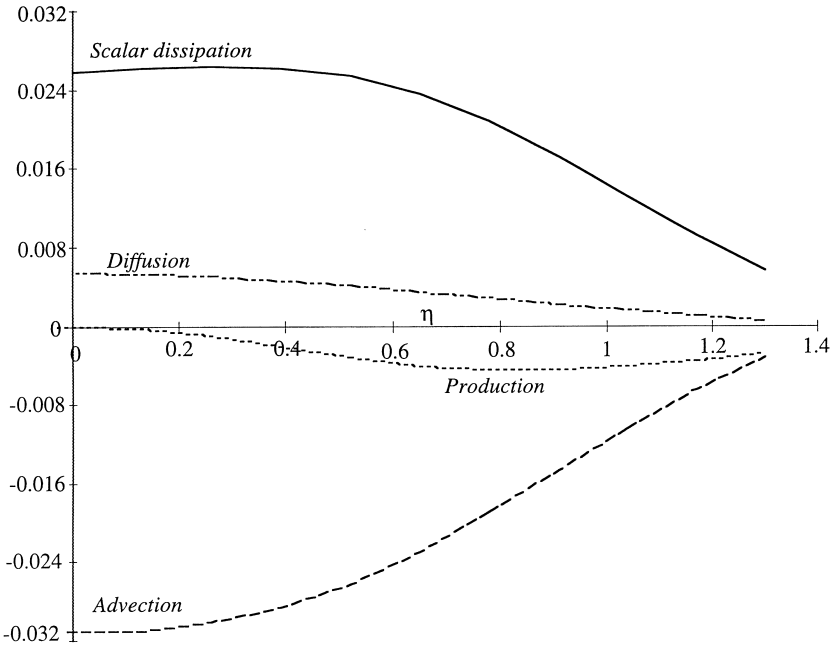

Fig. 12. Scalar variance budjet over the cross-section (in normalized values). – – – Advection: $\frac{1}{2}\bar{U}\frac{\partial\overline{c^2}}{\partial x}\times\frac{r_c}{\bar{U}\overline{c_c^2}}$; - - - production: $-\overline{cv}\frac{\partial\overline{C}}{\partial r}\times\frac{r_c}{\bar{U}\overline{c_c^2}}$; – · – diffusion: $-\frac{1}{r}\frac{\partial}{\partial r}\frac{r\overline{vc^2}}{r}\times\frac{r_c}{\bar{U}\overline{c_c^2}}$; ——— scalar dissipation: $-\varepsilon_c\times\frac{r_c}{\bar{U}\overline{c_c^2}}$.

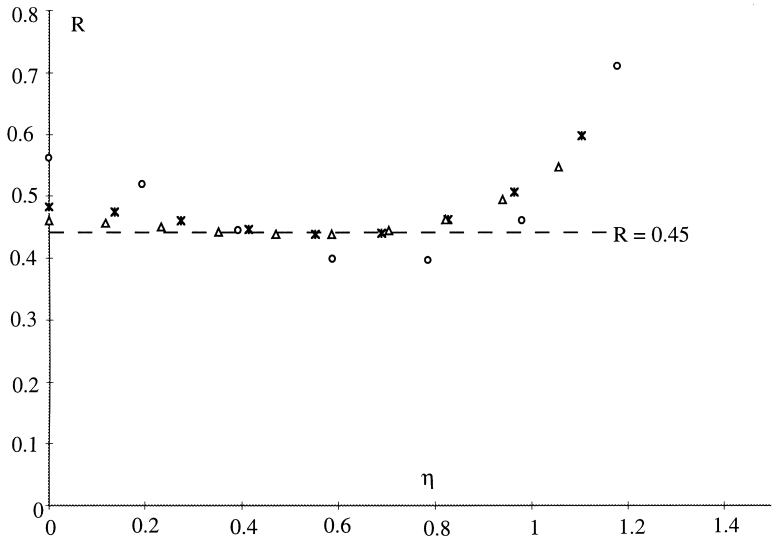

Fig. 13. Radial distribution of the scalar to velocity time scale ratio $R = (\varepsilon q)/(k\varepsilon_c)$. x/M: ○ 38; * 46; − 52.

For statistically homogeneous and quasi-isotropic turbulent flows, $\overline{u^2} = \frac{2}{3}k$, and then:

$$\lambda_u^2 = 10\nu\frac{k}{\varepsilon} \tag{21}$$

The Taylor microscale characterizing the scalar field is defined by Eq. (2):

$$\lambda_c^2 = 24\sigma\frac{q}{\varepsilon_c} \tag{22}$$

The ratio between the dynamic to scalar microscale is related to the Schmidt number Sc by:

$$\frac{\lambda_u^2}{\lambda_c^2} = Sc = \frac{5}{12}\frac{\nu}{\sigma}\frac{k}{\varepsilon}\frac{\varepsilon_c}{q} \tag{23}$$

Considering the Schmidt $Sc = \nu/s$, relation (23) yields the theoretical value of the scalar to velocity time scale ratio R:

$$R = \frac{5}{12} \times 0.41 \tag{24}$$

This value appears to be in very good agreement with the results found by analysis of the experimental data (R found experimentally is about 0.45). Moreover, as observed in the light of the experimental results, the ratio R appears constant in the streamwise direction and over the investigated cross-section. This rather good accordance between theoretical value and experimental observations of R validates the results obtained from the budjet over the concentration variance equation.

4. Self similarity of the fluctuating scalar field

The self similarity of both concentration and scalar variance fields has been checked experimentally. The consequences of this self similarity in the concentration variance equation (Eq. (8)) will be developed in this section. With the help of the self similar forms defined in Eqs. (9) and (13) for the mean concentration $\bar{C}$ and for the concentration variance $\overline{c^2}$, using relation (2) for ε_c, relation (19) for the model of the diffusion term and a turbulent diffusivity model for the closure of the turbulent mass flux $\overline{cv}$, Eq. (8) may be rewritten:

$$\frac{\partial^2 g}{\partial\eta^2} + \frac{\partial g}{\partial\eta}\left(\frac{1}{\eta} + \beta\eta\frac{D_t}{A_t}\right) + g(\eta)\left(4\beta\frac{D_t}{A_t} - 24\frac{\sigma}{\lambda_c^2}\frac{r_c^2}{A_t}\right) = -\frac{D_t}{A_t}\frac{\left(\bar{C}_c\right)^2}{\left(\overline{c^2}\right)_c}2\beta^2\eta^2 e^{-\beta\eta^2} \tag{25}$$

where $\beta = \ln(4)$, D_t is the turbulent diffusivity coefficient and $g(\eta)$ is defined by Eq. (13).

The conditions of self similarity requires constancy of the coefficients of Eq. (25). The coefficients which have to be constant are:

$$\frac{D_t}{A_t}, \quad 24\frac{\sigma}{\lambda_c^2}\frac{r_c^2}{A_t} \quad \text{and} \quad \frac{\left(\bar{C}_c\right)^2}{\left(\overline{c^2}\right)_c}$$

It has been demonstrated in Section 3.5 that the diffusivity A_t is a constant over the entire flowfield. The expansion length scale evolves as $r_c^2 \sim x/M$ which

involves that $\lambda_c^2 \sim x/M$. The turbulent diffusivity can be defined as in Ref. [10]:

$$D_t = \frac{1}{C_{c1}} \overline{v^2} \frac{k}{\varepsilon} \tag{26}$$

where $C_{c1} = 4.6$ is a constant determined with a similar grid turbulence experiment. Using the expression of coefficient A_t defined by the relation (19) the ratio D_t/A_t is:

$$\frac{D_t}{A_t} = \frac{1}{C_{c1} K_1} \times 0.7 \tag{27}$$

where K_1 is a constant defined by Eq. (19).

The turbulent diffusivity is almost constant over the flowfield, and its value is about D_t 10^{-4} m^2/s The value of A_t has been determined by using Eq. (27), and is compared with the experimental data reported in Fig. 11. Although the significant scatter of the experimental data, the agreement is good enough to be consider as consistent with the assumption that D_t/A_t is a constant. Relations (11) and (12) have shown that $\bar{C}_c^2$ and $(\overline{c^2})_c$ decrease as $(\frac{x}{M} - a)^2$, where a is a virtual origin. Although a difference of virtual origin, the ratio between $\bar{C}_c^2$ and $(\overline{c^2})_c$ tends to become constant as shown in Fig. 14, when x/M grows. As written in Eq. (10), the squared length scale r_c^2 evolves as x/M so that λ_c^2 should also vary as x/M. The real value of the scalar microscale λ_c can not be determined, since the molecular diffusivity is unknown. However, λ_c^2 is proportional to $\overline{c^2}/\varepsilon_c$ and the ratio $\overline{c^2}/(\varepsilon_c r_c^2)$ is reported in Fig. 14. A trend to stabilization at a constant value is also observed.

On the basis of the experimental data, the self similarity of the fluctuating concentration field has been demonstrated and the parameters necessary to solve the concentration variance equation have been fixed.

5. Conclusion

This paper has presented a budjet over the concentration variance equation, of a passive scalar discharging in a grid generated turbulent flow. All the terms of the concentration variance equation have been measured, except the concentration fluctuations dissipation rate, which has been deduced from the budjet of the equation. A gradient model of the triple correlation $\overline{vc^2}$ has been validated and the value of the turbulent diffusivity of the concentration variance has been determined. It has been demonstrated that the approximation advection dissipation is valid over the major part of the flowfield and that the streamwise decay of the concentration fluctuations can be written $\bar{U}\frac{\partial \bar{c}^2}{\partial r} \approx -\varepsilon_c$, similarly to the decay of the turbulent kinetic energy in the wake of a grid. The determination of the dissipation rate ε_c allows the calculation of the scalar to velocity time scale ratio. The self similarity of the concentration variance equation has been also investigated and all the conditions to obtain this self

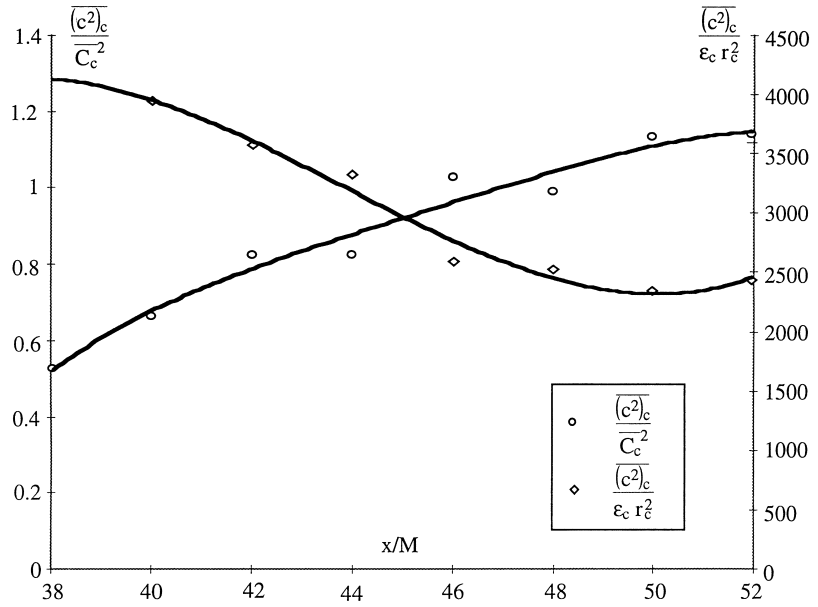

Fig. 14. Validation of the self similarity of the fluctuating concentration field.

similarity have been validated experimentally. Further experimental investigation would be valuable in homogeneous turbulent shear flows in order to validate closure concepts of the concentration variance equation.

References

[1] G.T. Csanady, Concentration fluctuations in turbulent diffusion, Journal of the Atmospheric Sciences 24 (1967) 21–28.

[2] J.O. Hinze, Turbulence, MacGraw-Hill, New York, 1975.

[3] G.K. Batchelor, J. Fluid Mech 5 (1959) 113.

[4] B.E. Launder, On the effect of a gravitational field on the turbulent transport of heat and momentum, J. Fluid Mech 67 (3) (1975) 569–581.

[5] B. E Launder, S.A. Samaraweera, Application of a second-moment turbulence closure to heat and mass transport in thin shear flows — two-dimensional transport, Int. Journal of Heat and Mass Transfer 22 (1979) 1631–1643.

[6] B.E. Launder, Heat and mass transport, in: Topics in Applied Physics, Turbulence, Springer-Verlag, Berlin, 1976.

[7] C.H. Gibson, W.H. Schwarz, The universal equilibrium spectra of turbulent velocity and scalar fields, J. Fluid Mech 16 (3) (1963) 365–384.

[8] I. Nakamura, Y. Sakai, M. Miyata, Diffusion of matter by a non-buoyant plume in grid-generated turbulence, J. Fluid Mech 178 (1987) 379–403.

[9] F. Lemoine, M. Wolff, M. Lebouch, Experimental investigation of mass transfer in a grid generated turbulent flow using combined optical methods, Int. Journal of Heat and Mass Transfer 40 (14) (1997) 3255–3266.

[10] F. Lemoine, Y. Antoine, M. Wolff, M. Lebouch, Mass transfer properties in a grid generated turbulent flow. Some experimental investigations about the concept of turbulent diffusivity, Int. Journal of Heat and Mass Transfer 41 (15) (1998) 2287–2295.

[11] F. Lemoine, M. Wolff, M. Lebouch, Simultaneous concentration and velocity measurements using combined laser-induced fluorescence and laser Doppler velocimetry: application to turbulent transport, Exp. in Fluids 20 (1996) 178–188.

[12] F. Lemoine, Y. Antoine, M. Wolff, M. Lebouch, Simultaneous temperature and 2D velocity measurements in a turbulent heated jet using combined laser-induced fluorescence and LDA, Exp. in Fluids 26 (1999) 315–323.

[13] D.A. Walker, A fluorescence technique for measurement of concentration in mixing liquids, J. Phys. E: Sci. Instrum 20 (1987) 217–224.

[14] S. Gaskey, P. Vacus, R. David, J. Villermaux, A method for the study of turbulent mixing using fluorescence spectroscopy, Exp. in Fluids 98 (1990) 137–147.

[15] J.C. Wyngaard, Boundary-Layer Methods 9 (1975) 44.

[16] D.B. Spadling, Concentration fluctuations in a round turbulent free jet, J. Chem. Engng. Sci 26 (1971) 95.